



# STRUCTURAL AND MULTIFERROIC PROPERTIES OF ER<sup>3+</sup>/BIFEO<sub>3</sub> NANOFERRITES

Monika<sup>1\*</sup>, S. K. Chaudhary<sup>1</sup>, Sunil Rohilla<sup>2</sup>, Praveen Kumar<sup>3</sup>, Varun Sangwan<sup>4</sup>

**Article History:** Received: 13.08.2023      Revised: 27.08.2023      Accepted: 28.09.2023

## Abstract:

In this work, we investigated rare earth driven structural, Dielectric, electro-strain-polarization and magnetic behaviors of Er<sup>3+</sup>/BiFeO<sub>3</sub> nano particles (NPs) synthesized via solid state route. From the XRD (X-ray Diffraction) measurements the average domain size was 23.7 nm as a result of the Er substitutions on the A-site in BFO, which also led to other structural modifications. The morphological studies were carried out via using FeSEM. The dielectric and complex impedance studies were carried out in the frequency range 2 MHz to 10 Hz at various temperatures. Significant decreases in the dielectric constant ( $\epsilon'$ ) have been noticed as frequency has increased, while increases in the  $\epsilon'$  have been recorded as the temperature has increased. The substitution of Er<sup>3+</sup> ions resulted in a considerable increase in saturation polarization ( $P_s$ ) is 1.884  $\mu\text{C}/\text{cm}^2$  and saturation magnetization ( $M_s$ ) is 3.27 emu/gm, as estimated by the ferro-electric hysteresis (P-E) loop and M-H hysteresis loop, correspondingly.

**Keywords:** Er substitution, Electro strain, Complex impedance, Ferroelectric, VSM.

<sup>1\*</sup>Department of Physics, Baba Mastnath University, Rohtak (India) -124021

<sup>2</sup>Department of Physics, C. R. S. University, Jind (India) -126102

<sup>3</sup>Department of Physics, Govt. College for Women, Tosham (India) -127040

<sup>4</sup>Department of Electronics and Communication, Delhi Technological University, New Delhi (India) -110042

**\*Corresponding Author:** Monika

<sup>\*</sup>Department of Physics, Baba Mastnath University, Rohtak (India) -124021,  
monikalohchab3333@gmail.com

**DOI:** 10.53555/ecb/2023.12.Si13.274

## 1. Introduction: -

Multiferroics are the nanomaterials that reveal more than one ferroic property, such as ferroelectricity, ferro-magnetism, and ferro-elasticity, among others. Bismuth ferrite (BiFeO<sub>3</sub>) is one of the mainly investigated multiferroic nanomaterials [1]. BiFeO<sub>3</sub> is a perovskite type oxide that exhibits both ferroelectric and anti-ferromagnetic ordering at 300 K, making it a promising material for various technological applications. BiFeO<sub>3</sub> has a huge Curie temperature (T<sub>c</sub>) ~ 1103 K with unique properties, making it useful for high temperature appliances [2-4]. Antiferromagnetic behavior in BiFeO<sub>3</sub> is due to unfilled d orbitals of Fe<sup>3+</sup> ions while, the ferroelectric behavior is shown due to the lone pair of electrons in 6s of Bi<sup>3+</sup> ions [5-6]. Most of the work reported in literature shows the presence of impurity phases in different samples [7]. Secondly leakage current shown by these Bi multiferroics is high but main issue related to low magnetization in bulk due to spiral modulated spin period of 62nm [8] thus limits the P-E loop to become saturate. These limitations restrict the application of bismuth multiferroic as a multifunctional device application. Several scientists tried different ways to overcome these shortcomings. These shortcomings can overcome up to a large extent by preparing nanoparticle of multiferroics at low temperature or by doping on Bi and Fe sites. In bismuth ferrites doping on Bi site (A site) is done via using rare earth elements having valency 3<sup>+</sup> such as Nd, Y, La etc. and alkaline earth elements having valency 2<sup>+</sup> such as Ba, Ca, Sr etc. to achieve enhancement in the properties of multiferroics via controlling their size, morphology, and surface area [4, 9-10]. However a number of scientist worked on Er doped BiFeO<sub>3</sub> but on reviewing literature it is noticed that researchers considerably focuses on the study related to magnetic property but detailed study on dielectric and electro-strain properties are still a matter of research. So, the present study investigates in detail on structural, electric transport, electro strain and magnetic properties of Er substituted BFO nano-ferrites.

## 2. Results and discussions:

### 2.1 Structural and phase Characterization:

The XRD pattern (From figure 1) of Bi<sub>1-x</sub>Er<sub>x</sub>FeO<sub>3</sub> (x = 0.20 (E4)) confirms that the crystallographic structure of the doped compositions is a distorted rhombohedral structure (space group R3c), which is the same as that of the parent BFO crystal system (Card No. 86-1518) [10]. The observed shift and change in the XRD blueprint of the doped compositions indicates that the substitution

of Er in BiFeO<sub>3</sub> has led to structural changes in the material. This is due to persuade of dissimilar ionic radii among the doped ion and parent metal ion. The diffraction peaks show an obvious shift toward a higher degree (2θ), which is due to vaguely lower ionic radius of Er (1.001Å) compared to bismuth (1.03 Å). This confirms that Er ions have been effectively doped into all samples of BiFeO<sub>3</sub>. Using Scherer's Formula, the usual crystalline (domain) diameters of the samples were determined [11]:

$$D = \frac{K\lambda}{\beta \cos\theta} \dots\dots\dots (1)$$

In this formula, K~0.9 is the shape factor, wavelength of the X-ray is λ, β is FWHM, and angle of diffraction is θ. With an augment in dopant concentration, the mean crystalline size of all Er/BiFeO<sub>3</sub> samples was found 23.7 nm.

### 2.2 Morphological Analysis:

The figure 2 describes the results of field emission scanning electron microscope (FESEM) analysis of E4 samples modified with different concentrations of Er. The FESEM images show that the samples have a polycrystalline structure, and their particle sizes decrease with increasing Er concentration. From the figure 2 it is clear that these samples are polycrystalline in nature, gyroid, glowing ordered like shapes and agglomerated because of high energy chemical reaction [12]. The asymmetrical distribution of particles might persuade the structural, multiferroic, and electro strain properties of the multiferroics.

### 2.3 Dielectric Analysis:

The dielectric constant (ε') is an indicator of the ability of a nanomaterial to accumulate the electric energy in an E-field. In figure 3, it could be seen that the ε' values augmented with decreasing frequency at all measured temperatures for all Er/BFO compositions. This behavior is typical for ferroelectric materials, where the polarization changes direction as the electric field direction changes [13-14]. At lower frequencies, there is more time for the polarization to switch direction, resulting in a higher ε' value. Additionally, the ε' values decrease with increasing temperature at all measured frequencies for all Er/BFO compositions. This behavior is consistent with the reduction of the ferro-electric transition temperature with escalating temperature. The values of Dielectric constant (ε') are estimated via using the formulas [14]:

$$\epsilon' = \frac{1}{\omega\epsilon_0} \left( \frac{Z''}{Z'{}^2 + Z''{}^2} \right) \dots\dots\dots (2)$$

Where  $Z'$  and  $Z''$  are the real and imaginary factor of  $Z$ ,  $\omega$  is frequency and  $\epsilon_0$  is permittivity of free space. Furthermore, the value of  $\epsilon'$  in all the synthesized Er/BFO compositions is sturdily reliant on frequency and temperature. The  $\epsilon'$  gradually increases with rising the temperature due to the presence of thermally activated charges and hopping conduction [15].

#### 2.4 Electronic transport phenomenon of grains and grain boundaries:

Based on the complex impedance ( $Z$ ) analysis, it can be inferred that the dielectric relaxation behavior of the E4 samples of Er/BFO was studied. The Nyquist plots (As per figure 4), which show the variation of complex impedance (imaginary part v/s real part of  $Z$ ), were plotted for each composition at various temperatures in the range of frequency from 2 MHz to 10 Hz. The semicircular shape of the Nyquist plots is indicative of the grains in the materials [16]. At lower temperatures, all the compositions of Er/BFO exhibit a huge insulating nature, as indicated by the semicircular shape of the Nyquist plots.

#### 2.5 Electrical Ac conductivity Analysis:

The study investigated the relationship between relaxation and conduction mechanism and also the effect of Er doping in BiFeO<sub>3</sub> nonmaterials by determining AC conductivities as the variation of frequency from 2 MHz to 10 Hz at variety of temperatures (figure 5). The ac conductivity was measured using the relationship:

$$\sigma_{AC}(\omega) = \omega \epsilon_0 \epsilon' \tan \delta \dots \dots \dots (3)$$

Where,  $\epsilon_0$  is the free space permittivity, and  $\tan \delta$  is the dielectric loss. The increase in AC conductivities with increasing frequency of the functional field is because of the hopping of charge carriers, thus envisaged by Koop's phenomenological theory [17]. Moreover, AC conductivities increases with temperature due to the contribution of charge deficiencies, like ionization of O<sub>2</sub> vacancy and thermally triggered charge carriers, which contribute to the conduction and relaxation correlation in BiFeO<sub>3</sub> samples [18].

#### 2.6 Ferro-electric and electric field driven strain studies:

The ferroelectric hysteresis (P-E) measurements carried out (figure 6) for E4 samples BFO at 300 K and investigated the E-field obsessed strain behavior as a application of E-field (kV/cm) at 100Hz (Figure 6). The P-E loops for pure BFO are difficult to obtain because of the huge leakage

current and giant coercive field ( $E_c$ ), which is also observed in samples with defects dipoles and conducting nature [18]. However, the rare earth modified BFO's are more resistive in scenery because of squat charge effect, which leads to the penning of the P-E loops. The estimated value of remanent polarization ( $2P_r$ ) to be found in the range 1.64  $\mu\text{C}/\text{cm}^2$ , respectively, for E4 samples of BFO

#### 2.7 VSM Analysis:

The M-H hysteresis curves (figure 7) for the Er doped BFO samples reveal that the curves barely saturate near 2000 Oe and stay saturated yet the M-field is enlarged up to 6000 Oe. This suggests that the samples are able to withstand high magnetic fields without losing their magnetic properties. The saturation magnetization ( $M_s$ ) values for the Er/BFO samples increase with the concentration of Er dopant, with values of 1.884 emu/gm observed for E4 samples. The exchange interaction between the substituted ions Er and Fe and the repression of the canted spiral spin arrangement might be accountable for the increased levels of magnetization in the Er-doped BiFeO<sub>3</sub> samples [19].

### 3. Conclusions

In essence, we fruitfully synthesize Bi<sub>1-x</sub>Er<sub>x</sub>FeO<sub>3</sub> ( $x = 0.20$  (E4)) or Er/BFO nanoferrites using a solid state procedure and examine the influence of Er<sup>3+</sup> substitution on the BiFeO<sub>3</sub> for electric field encouraged strain and multi-ferroic properties of the material. XRD measurements showed a structural change from rhombohedral (R3c) to orthorhombic (Pnma) symmetry. As per Scherrer's formula, the mean crystallite size for Er/BFO nanoferrites was 23.7 nm. The occurrence of abnormally leaning defective dipoles and Er<sup>3+</sup> substitution results in a rise in saturation polarization ( $P_s$ ) (at  $\omega = 100$  Hz) and saturation magnetization ( $M_s$ ) as an efficacy of the functional field. The values of saturation polarization ( $P_s$ ) and magnetization ( $M_s$ ), respectively, have augmented were 1.884  $\mu\text{C}/\text{cm}^2$  and 3.27 emu/gm. The energy storage density has increased up to 5.582  $\text{mJ}/\text{cm}^3$ . This research should support and further auxiliary work based on strain convincing memory effect and rare earth modified multi-ferroics for energy storage applications, thus might be functional in the field of green energy and actuators.

**Acknowledgment:** The authors are also grateful to the Head, Department of Physics of BMU rohtak and CRSU Jind for providing facilities and

essential support to the researchers. The authors didn't have any financial assistance for this work.

**Credit Authorship Contribution Statement:**

**Monika:** Methodology, Data curation, and Writing-original draft, **S. K. Chaudhary:** Conceptualization, Validation, Resources, supervision; **Sunil Rohilla:** Writing - review & editing, supervision; **Praveen Kumar:** Software, instrumentation; **Varun Sangwan:** Validation, Review & editing.

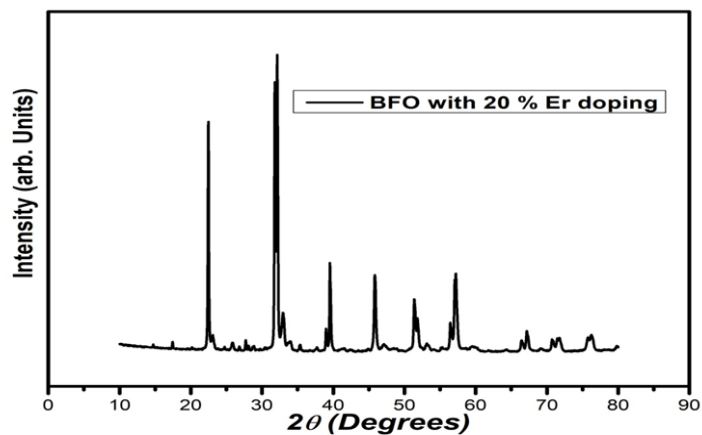
**Conflict of Interest:** The authors state that they have no known competing financial interests or personal ties that could have influenced the research presented in this study.

**Reference:**

1. H. Schmid et al., Multi-ferroic magnetoelectrics, *Ferroelectrics* 162 (1994) 317-338.
2. D. Lebeugle et al., Room-temperature coexistence of large electric polarization and magnetic order in BiFeO<sub>3</sub> single crystals, *Physical Review B* 76 (2007) 024116.
3. X L Xu, Xing-Liang et al., Enhanced multiferroic properties in Er and Mn Co-doped BiFeO<sub>3</sub> nanoparticles, *Journal of Superconductivity and Novel Magnetism* 35.7 (2022): 1961-1966.
4. I. Sosnowska et al., Spiral magnetic ordering in bismuth ferrite, *Journal of Physics C: Solid State Physics* 15.23 (1982): 4835.
5. W. Eerenstein et al., Multiferroic and magnetoelectric materials, *Nature* 442 (2006) 759.
6. H. Dai et al., The effect of ion doping at different sites on the structure, defects and multiferroic properties of BiFeO<sub>3</sub> ceramics, *Journal of Alloys and Compounds* 734 (2018): 60-65.
7. C. Lu and Jun-Ming Liu, DyMnO<sub>3</sub>: A model system of type-II multiferroics, *Journal of Materiomics* 2(2016)213-224.
8. M M Rhaman et al., Dielectric, ferroelectric and ferromagnetic properties of samarium doped multiferroic bismuth ferrite, *Materials Research Express* 6.12 (2019): 125080.
9. G. Catalan et al., Physics and applications of bismuth ferrite, *Advanced Materials* 21 (2009) 2463-2485.
10. F Sanchez-De Jesus et al., Enhanced ferromagnetic and electric properties of multiferroic BiFeO<sub>3</sub> by doping with Ca, *Journal of Alloys and Compounds* 824 (2020): 153944.
11. Y Ahn et al., Multiferroic properties and ferroelectric domain structures of Yb-doped BiFeO<sub>3</sub> thin films on glass substrates, *Physica B: Condensed Matter* 558 (2019): 24-27.
12. X. Zhang et al., Effect of Eu substitution on the crystal structure and multiferroic properties of BiFeO<sub>3</sub>, *Journal of alloys and compounds* 507.1 (2010): 157-16.
13. R. Dahiya et al., Structural, magnetic and dielectric properties of Sr and V doped BiFeO<sub>3</sub> multiferroics, *Journal of Magnetism and Magnetic Materials* 385 (2015): 175-181.
14. P. Kumar and P. Chand, Structural, electric transport response and electro-strain-Polarization effect in La and Ni modified bismuth ferrite nanostructures, *Journal of Alloys and Compounds* 748 (2018)504-514.
15. P. Chand, S. Vaish and P. Kumar, Structural, optical and dielectric properties of transition metal (MFe<sub>2</sub>O<sub>4</sub>; M= Co, Ni and Zn) nanoferrites, *Physica B: Condensed Matter* 524 (2017) 53-63.
16. R Ramadan, Study the multiferroic properties of BiFeO<sub>3</sub>/Ni<sub>0.1</sub>Fe<sub>2.9</sub>O<sub>4</sub> for heavy metal removal, *Applied Physics A* 129.2 (2023): 125.
17. M A Mosa et al, Enhanced multiferroic properties in Ba and Sm co-doped BiFeO<sub>3</sub> ceramics, *Journal of Materials Science: Materials in Electronics* 33.33 (2022): 25089-25102.
18. A S Priya et al., Tunable Optical and Multiferroic Properties of Zirconium and Dysprosium Substituted Bismuth Ferrite Thin Films, *Molecules* 27.21 (2022): 7565.
19. B S Kar et al., Effects of lanthanum dopants on dielectric and multiferroic properties of BiFeO<sub>3</sub>-BaTiO<sub>3</sub> ceramics, *Journal of Alloys and Compounds* 861 (2021): 157960.

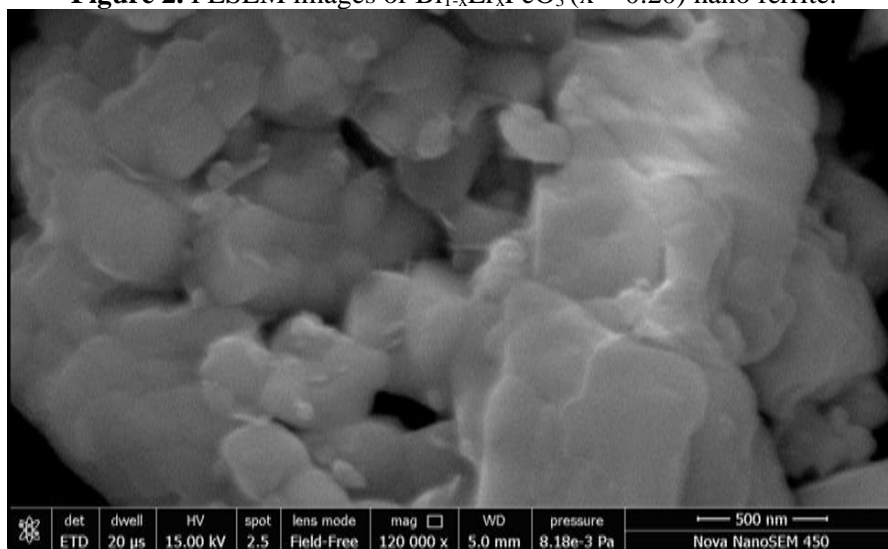
**Figure captions**

**Figure 1.** XRD patterns of  $Bi_{1-x}Er_xFeO_3$  ( $x = 0.20$ ) nano ferrite samples at room temperature.



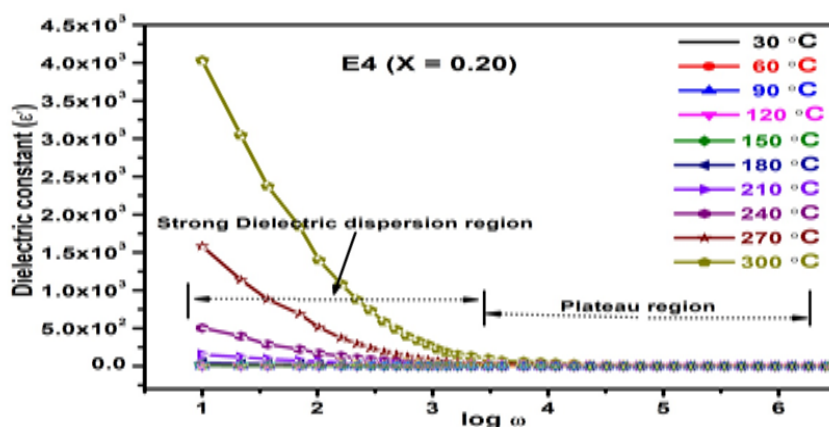
**Figure 1.**

**Figure 2.** FESEM images of  $Bi_{1-x}Er_xFeO_3$  ( $x = 0.20$ ) nano ferrite.



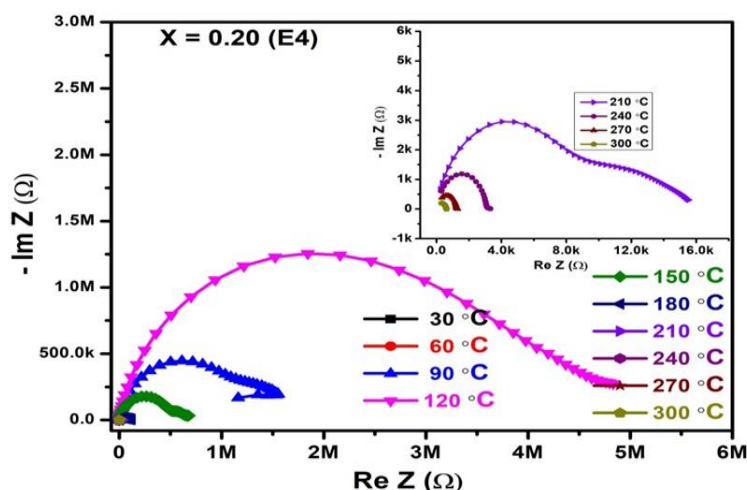
**Figure 2**

**Figure 3.** Variation of dielectric constant with frequency at various temperatures for  $Bi_{1-x}Er_xFeO_3$  ( $x = 0.20$ ) nano ferrites.



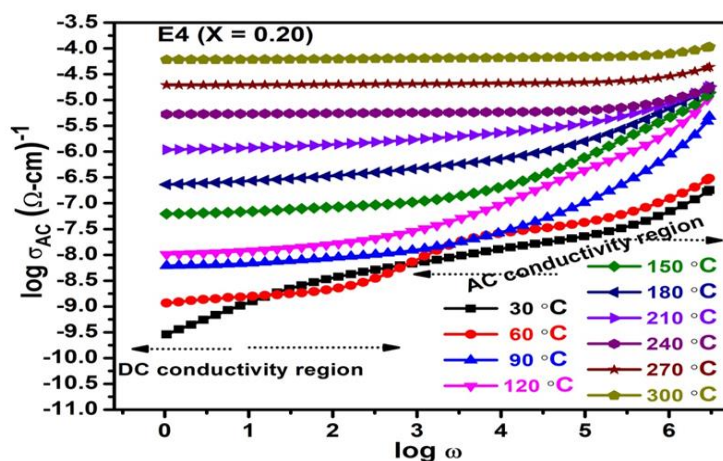
**Figure 3**

**Figure 4.** Nyquist plot (Cole-Cole) of  $Bi_{1-x}Er_xFeO_3$  ( $x = 0.20$ ) nano ferrites.



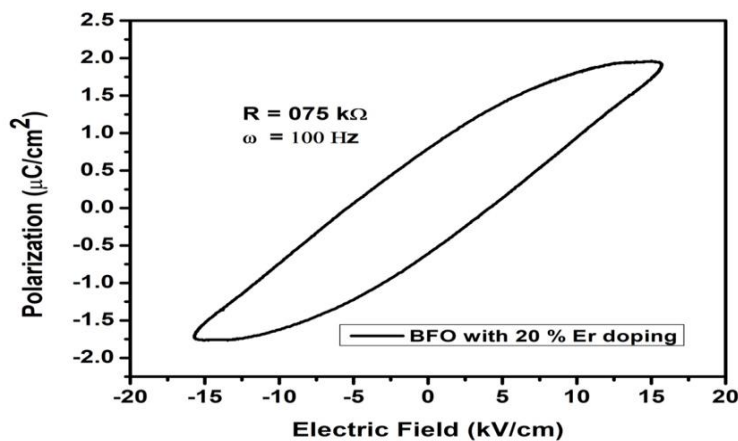
**Figure 4.**

**Figure 5.** Variation of AC conductivities with frequency at various temperatures for  $Bi_{1-x}Er_xFeO_3$  ( $x = 0.20$ ) nano ferrites.

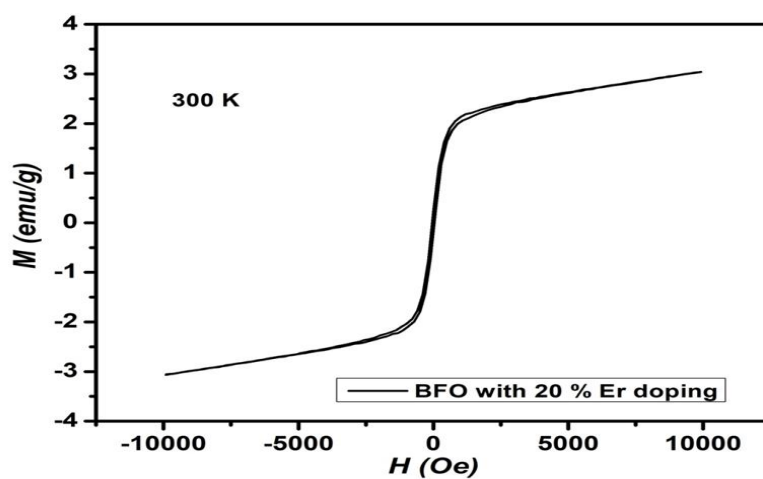


**Figure 5**

**Figure 6.** P- E hysteresis loops of  $Bi_{1-x}Er_xFeO_3$  ( $x = 0.20$ ) nano ferrites as a function of frequency for an applied electric field at Room temperature.



**Figure 6**

**Figure 7.** Room temperature M-H hysteresis loops of  $\text{Bi}_{1-x}\text{Er}_x\text{FeO}_3$  ( $x = 0.20$ ) nano ferrites.**Figure 7.**